Testing a free-stream turbine a in real turbulent tidal flow

A. Sentchev*[1], M.Thiébaut*[2], François G.Schmitt†[3],

*Laboratoire d'Océanologie et de Géosciences (UMR 8187), Université du Littoral - Côte d'Opale,
32 avenue Foch, 62930 Wimereux, France.
†Laboratoire d'Océanologie et de Géosciences (UMR 8187), CNRS,
28 avenue Foch, 62930 Wimereux, France.
[1]alexei.sentchev@univ-littoral.fr, [2]maxime.thiebaut@univ-littoral.fr,[3]françois.schmitt@cnrs.fr

Abstract :

A vertical axis tidal turbine (VATT) of the Dutch company "Water2Energy", mounted on a surface platform, was tested during several weeks in real sea conditions in a tidal estuary - the Sea Scheldt, Belgium. Velocity measurements were performed to estimate the major turbulent properties of the tidal flow at the experimental site, to evaluate the tidal turbine performance, and to quantify the effect of turbulence on the output power. The optimal performance (C_p) of the turbine was founded to be 0.42 in the velocity range 1.1−1.2 m/s. The results show that the dissipation rate, ϵ, and turbulent strength, σ_u are tightly related with the magnitude of the output power variability. It was demonstrated that tidal turbine responds more actively to turbulence on scales similar to the rotor diameter.

Keywords : Tidal turbine testing - Turbulence - Power coefficient - Estuary

1 Introduction

In recent years, full-scale prototypes of tidal-stream turbines have been used as pre-commercial demonstrators in many countries. Advancements in hydrokinetic power conversion from tidal currents require detailed understanding of the fluid velocities surrounding devices, in particular the turbulence. Experience in the wind energy industry indicates that turbulence is the primary cause of fatigue and thus determines the life expectancy of a turbine. For this reason, the characterization of the natural turbulence has been identified as a priority for tidal energy site assessment [1].

However, the accurate assessment of turbulent properties of a powerful tidal flow is not trivial due in part to a wide range of length and time scales that exist in a high Reynolds number flow. Moreover, turbulence is highly intermittent and bursts of energy can occur at irregular time intervals and be localized in space.

Faced to difficulties in characterizing the turbulent properties of the flow in a broad scale, analysis of a possible link between the "local turbulence strength" and tidal energy conversion device performance is often done using a theoretical framework of energy multifractal cascades [2], experimental approach in a flume tank [3, 4], and modelling approach [5, 6].

A lot of research efforts have been focused on understanding of the effect of ambient turbulence

intensity on the devices performance. Experiments in flume tank and modelling allowed to optimize the system design and performance of a single device or an array of devices [7, 8, 3].

In spite of these and many other studies, a number of fundamental problems remain poorly understood. For example, a central question is the range of scales in the approach turbulent flow and how this reaches interaction of turbulence with a device modifies its ability to produce power. This question remains totally unexplored in case of a full-scale or reduced-scale device operating in periodic (tidal), highly energetic, and highly turbulent flow.

The number of scientific publications reporting the results of full-scale device performance assessment is by far insufficient. MacEnri et al. [9] documented a determining effect of tidal current speed and turbulence strength on the flicker performance of the MCT SeaGen 1.2 MW tidal energy converter. Jeffcoate et al. [10] investigated the performance of a 1/10 scale tidal turbine (1.5 m diameter) in both steady state and real sea flow conditions. They documented a global decrease and strong variations of the performance in turbulent tidal flow at the experimental site in Strangford Narrows (UK). However the turbulent properties of the flow at site were not estimated and a link with the power production was not established.

A common metric that is used to characterize a turbulent flow is the dissipation rate ϵ, of the turbulent kinetic energy (TKE). In the inertial sub-range, which separates the large production scales from the small dissipation scales, the energy associated with the velocity fluctuations is independent of viscosity and only related to the dissipation rate and eddy size. The latter represents another useful metric characterizing the turbulence.

In many studies focusing on resource assessment at tidal energy sites, the turbulent properties of the flow are estimated using in situ measurements of current velocity by an acoustic Doppler current profiler (ADCP) or acoustic Doppler velocimeter (ADV). Because of different sampling rates, both instruments are capable of resolving different parts of the inertial sub-range which spans several orders of magnitude, typically from 1 mm to 10 m.

ADCP is probably the most used instrument for tidal energy site characterization and the number of results reported grows every year (e.g. [11, 12, 13]). It provides estimates of flow variability in the whole water column in extended frequency band covering time scales from a second to sub-tidal. However due to relatively high noise level and diverging beams, ADCPs are not capable to provide reliable estimates of turbulent properties derived from velocity records at ranges more than several meters apart from the transducers. Thus the inertial sub-range can be resolved for length scales larger than $\sim$ 1 m, which can be acceptable only for an estimate of an average dissipation rate. Furthermore, the variation of ϵ as a function of flow speed and water depth can be analyzed using the ADCP measurements [11, 12, 14].

For observations of smaller length scales ADV measurements are required. They are much more appropriate for ambient turbulence characterization as velocity recording is performed at high sampling rate (up to 64 Hz) by converging beams at a fixed depth. Since the last several years, ADV records have been extensively used for estimating turbulence parameters (dissipation rate, turbulence intensity, coherence length) at tidal energy sites (e.g. [11, 15, 13, 16]).

In this paper, the results of free-stream tidal turbine tests conducted in a tidal estuary (the Sea Scheldt, Belgium) are presented. Tidal flow velocity time series were recorded upstream the turbine by a downward-looking ADCP and ADV. The output power generated by tidal turbine was also recorded. The acquired data allowed to estimate the major turbulent properties of the tidal flow at the experimental site, to evaluate the tidal turbine performance, and to quantify the effect of turbulence on the output power.

2 Data and methods

2.1 Experimental site

The experimental site, located west of Antwerp (Belgium), was designed to receive free stream Darrieus type turbines for testing in real conditions in a tidal estuary - the Sea Scheldt, during a period of several months. Two turbines, manufactured by Water2Energy (W2E) and Blue Energy Canada (BEC) companies, have been tested at site. Results reported in this study concern only one turbine - W2E.

A floating pontoon (3 m x 39 m) was installed in the middle of the Sea Scheldt between two piles oriented in the streamwise direction (Fig. 1). At pontoon location, the river width and the mean depth are approximately 300 m and 8 m. The tidal turbine was installed at a side of the pontoon for a total period of eight weeks starting from the end of October 2014.

The flow regime in the estuary is strongly dominated by tides of semi-diurnal period. The tidal range is of the order of 6 m with a slight fortnight modulation. Tidal current velocities attain the maximum values of 1.5 m/s and 1.9 m/s during neap and spring tide respectively. A typical cycle of tidal flow evolution is shown in Fig. 2. Flood tide lasts slightly less than 7 hours and ebb tide approximately 5.5 hours. The slack water duration, after the current reversal (CR) of low water (LW), is very short and the tidal current velocity changes from 0.8 m/s to - 0.8 m/s in less then one hour. The mean ebb flow velocity is 0.2 m/s higher than the mean flood flow velocity. This difference is caused by a particular shape of the velocity curve with a pronounced saddle point at flood flow (Fig. 2).

2.2 Velocity measurements

Current velocities were recorded simultaneously by ADV and ADCP, both mounted on a fixed frame and installed on a steel beam at the extremity of the pontoon upstream the turbine (Fig. 3). ADCP was aligned with the middle line of the turbine whereas ADV was out of line by approximately 1 m.

A 1.2-MHz downward-looking four-beam broadband RDI ADCP was sampling the current velocity during several tidal periods of turbine test runs. The instrument, operating in fast pinging mode, recorded one velocity profile per second. Each one-second velocity record was an average of three short pulse measurements (sub-pings) providing the accuracy of velocity acquisition better than 0.04 m/s (according to RDI PlanADCP software specification). Velocities were recorded in beam coordinates with 0.25 m vertical resolution (bin size), starting from 0.8 m below the surface (midpoint of the first bin). The

Figure 1: Experimental pontoon installed in the tidal estuary (Sea Scheldt, west of Antwerp) for tidal turbine tests in real conditions (left panel). A vertical axis tidal turbine of the Dutch company "Water2Energy" mounted on a surface floating platform and installed at a side of the pontoon (right panel).

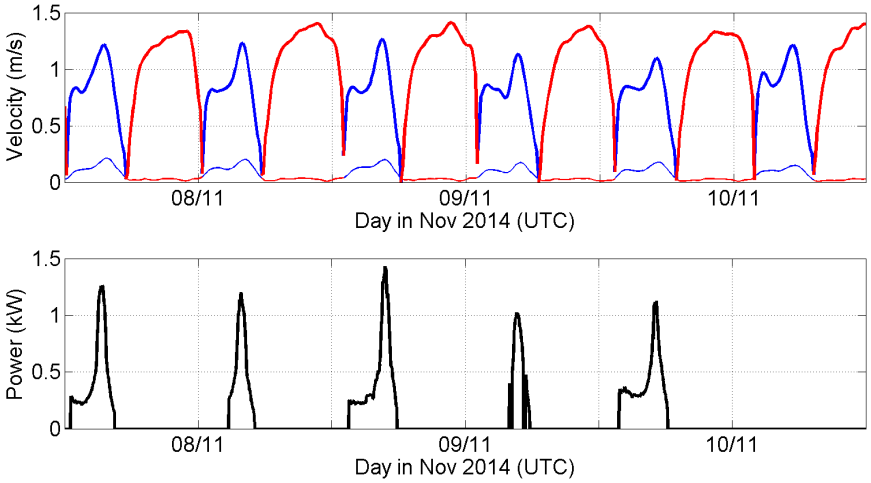

Figure 2: Ten minute averaged velocity time series in the surface layer 2-m thick measured by ADCP in November 2014 during the turbine test in the Sea Scheldt (upper panel). Thick and thin lines represent the streamwise and spanwise velocity components. Red and blue match ebb and flood flow velocities. Lower panel: The power (ten minute averaged) generated by the W2E turbine during the flood flow for the same period.

velocity data provided by ADCP were used for tidal flow characterization, comparison with ADV data and evaluation of the kinetic power available in the flow. A total of three deployments were performed at test site using identical configuration. The longest period of data acquisition lasted 11 tidal cycles (7-11 Nov, 2014).

An ADV, installed next to ADCP, was recording 3 components of the flow velocity at $\sim$ 1 m depth. The measurements covered different tidal current regimes: strong ebb and flood flow with velocity above 1.2 m/s and also a flow reversal. A total of four deployments were performed at test site. During one deployment, two ADV recorded simultaneously velocities with sampling frequency of 16 and 32 Hz. The distance between the tidal turbine and ADV and ADCP is estimated as $9D$ (18 m) with D being the turbine diameter (Fig. 3). The recorded horizontal velocities (eastward and northward components) were projected on along- and cross-stream axes of the river flow. Time series of the streamwise velocity (u component) and spanwise velocity (v component) were thus generated for further analysis. The quality of the data recorded by ADV and ADCP was very good and the data did not require any filtering.

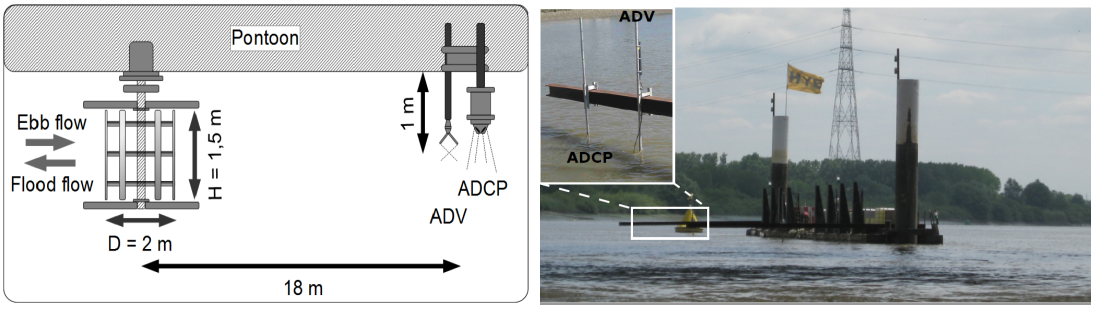

Figure 3: Schematic of the experimental setup in the Sea Scheldt (left panel) and the view of ADV and ADCP installed on a steel beam at the extremity of the pontoon downstream the turbine (right panel).

2.3 Tidal Current Turbine

A Darrieus type Vertical Axis Tidal Turbine (VATT) of "Water2Energy" company (Netherlands), was installed at a side of the pontoon, one meter apart, and was tested during eight week period in winter 2014. The device is 1.5 m high (H), 2 m diameter (D), four blades, pitch controlled turbine, with a capability to produce power during the entire tidal cycle including ebb and flood flow, and a cut-in-speed of 0.5 m/s. The output power and rotor velocity were recorded at 100 Hz acquisition frequency.

2.4 Metrics for assessing the mean and turbulent flow properties

The experiment was designed to assess the turbine performance and to study a dynamically rich interaction of a fully developed turbulent flow with the turbine. The tidal flow variability was characterized using the velocity time series provided by ADV and ADCP. The range of velocity variations, the occurrence of velocity values, and current asymmetry were estimated. The major turbulence properties of the flow were also quantified.

The turbulence intensity is conventionally used to quantify the ambient turbulence level. This metric has been shown to correlate with the extreme loads exerted on the turbine which is the major source of fatigue. Considering the streamwise velocity component u, the turbulence intensity in the direction of u is defined as the ratio of velocity fluctuations to the mean (typically 10-minute averaged) velocity $< u >$:

$$I_u = \frac{\sigma_u}{< u >} \tag{1}$$

The standard deviation of velocity, σ_u, also called the turbulence strength, is another quantity characterizing the turbulence.

The dissipation rate ϵ is estimated using the power spectrum $E(k)$ of the velocity time series assuming Kolmogorov relationship of the local isotropic turbulence [2, 17]:

$$E(k) = C\epsilon^{2/3}k^{-5/3} \tag{2}$$

where C is a constant ($C \simeq 1.5$) and k the wavenumber. Frequency and wavenumber are related with the averaged over the analyzed period velocity magnitude U, such as: $k = 2\pi f/U$. Thus, the dissipation rate can be estimated from the power spectrum as [11]:

$$\epsilon = \left(\frac{C_0}{C}\right)^{3/2} \left(\frac{2\pi}{U}\right)^{5/2} \tag{3}$$

where C_0 is a constant such as $E(f) = C_0 f^{-5/3}$ is the best fit estimated over the inertial sub-range.

The value of ϵ allows to determine two other flow scaling properties: the energy injection scale L (the integral scale) and the Kolmogorov dissipation scale η defined by:

$$L = \frac{\sigma_u^3}{\epsilon} \tag{4}$$

and

$$\eta = \left(\frac{\nu^3}{\epsilon}\right)^{1/4} \tag{5}$$

where ν is the kinematic viscosity of water (ν = 1.5 10^{-6} m^2/s).

3 Results

3.1 Tidal dynamics, turbulent strength and intensity

The water dynamics in the Sea Scheldt is by far dominated by tides. The maximum tidal range at test site location is of the order of 6 m with a small diurnal inequality. The tidal flow is predominantly alternative. The current velocity vector draws an ellipse whose major axis is aligned with the flow direction. A low eccentricity of the tidal current ellipse allows to consider two velocity components in a frame related to the main river axis. In the following, the analysis will concern the streamwise velocity component. On average, the streamwise velocity exceeds the spanwise velocity by an order of magnitude (Fig. 2).

In the surface 2-m thick layer, the flood and ebb flow direction reveals a light misalignment (direction asymmetry) of the order of 7°. The direction asymmetry disappears at the mid-depth ($\sim$ 5-6 m), and becomes negative: -7°, in the bottom layer (results not shown). The observed counter-clockwise current vector rotation is caused by the bottom friction.

An overall asymmetry of the current velocity, a, defined as the ratio of the mean velocity during flood tide to the mean velocity during ebb tide, was found close to 0.75 and revealed variations during different ADCP surveys. On average, in the surface layer, the mean ebb flow velocity exceeds 1 m/s whereas the mean flood flow velocity is less than 0.8 m/s. During specific hydrological conditions, the peak flood flow velocity can exceed that of ebb flow velocity by up to 0.2 m/s, but such situations are irregular. The highest velocity values are reached at low water (LW) on ebb tide and at high water (HW) on flood tide.

Current velocity records provided by ADV during the period preceding the turbine test runs were chosen for assessing the turbulent properties of the tidal flow in more detail. Due to low noise of ADV measurements, these velocity data were preferred to ADCP data. The velocity record (streamwise component) during a typical tidal cycle is shown in Fig. 4. The level of ambient turbulence in a natural tidal flow at the experimental site is characterized by estimating two quantities: the turbulence strength, σ_u, and turbulence intensity, I_u. Small values of the spanwise velocity v, compared to the streamwise component u (Fig. 3), cause an artificial increase of the turbulent intensity I_v (Tab. 1) and make the total intensity I_{uv} unsusable. For this reason, analysis of the turbulence evolution and estimation of I_u were performed for periods with velocity higher than 0.8 m/s. The results, summarized in Tab. 1, reveal that during three characteristic periods, shown in Fig. 4a and covering the strongest flood and ebb tidal currents, the level of ambient turbulence in the flow does not change significantly. The mean turbulence intensity varies within a narrow range, from 5 to 7%.

On the contrary, the turbulence strength shows larger variation during the tidal cycle, in particular when the velocity rises from 0.8 m/s to more than 1 m/s (Fig. 4 and Tab. 1). The turbulence strength characterizes the magnitude of high frequency velocity fluctuations. For strongest flood and ebb current (u > 1 m/s), typical σ_u values reach 0.07 m/s, compared to σ_u = 0.04 m/s for velocity ranging from 0.8 to 1 m/s (Tab. 1). The turbulent intensity, derived from ADCP data, appeared overestimated by 20-30%, compared to respective quantities derived from ADV. The reason is a larger noise level of ADCP measurements, already documented in previous studies (e.g. [11]).

3.2 Scaling properties of the tidal flow

The magnitude of high frequency velocity variations (Fig. 4) evidences a different level of ambient turbulence during different stages of a tidal cycle. This difference does not clearly appear in estimates

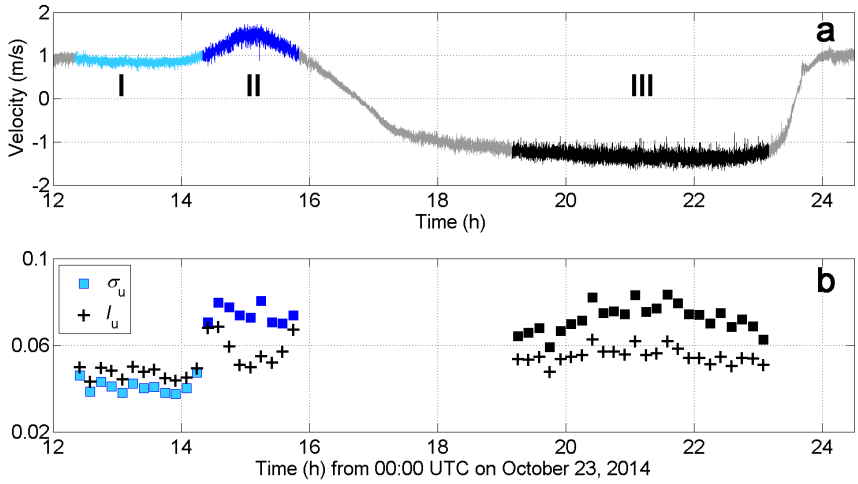

Figure 4: (a) Current velocity (streamwise component u) recorded by ADV at 16 Hz during a tidal cycle on October 23, 2014. (b) Turbulence intensity I_u and turbulence strength σ_u evolution during three specific periods of the tidal cycle used for detailed analysis and numbered I to III in (a). Light, dark blue and black colours match the property variations during the respective periods.

of I_u. Only the turbulent strength reveals a change in the local turbulence level which is related to the flow regime evolution.

A metric commonly used to characterize turbulence in a flow is the dissipation rate, ϵ. It can be quantified through a spectral analysis of velocity time series, in particular in the inertial sub-range. Here, the energy associated with the velocity fluctuations is related to the dissipation rate and eddy size. Both quantities can be deduced from the spectral representation of velocity time series.

Fig. 5 shows the power spectral density (PSD) of velocity recorded by ADV during three successive periods of a tidal cycle in the afternoon, on October 23, 2014. Quite similar results are obtained for other ADV survey periods in 2015. Each short sub-period, numbered I, II, and III within a tidal cycle, has different duration: 2, 1.5 and 4 hours respectively (Fig. 4a).

For each period, three frequency sub-ranges can be identified in Fig. 5: the low frequency sub-range ($f < 10^{-1}$ Hz), the inertial sub-range, limited by 10^{-1} Hz and 4 Hz, and high frequency sub-range ($f >$ 4 Hz) where the PSD curve is influenced by the noise in the data. Three fundamental properties of the turbulent flow: the dissipation rate ε, energy injection scale L, and Kolmogorov scale η, are estimated from the PSD distribution for each of three periods of ADV survey (Fig. 5) and summarized in Tab. 2. Two latter quantities are related to characteristic size of motions in the tidal estuary: size of eddies generated in a (assumed homogeneous) turbulent flow, and the smallest scale at which turbulent motions dissipate as a heat under the affect of viscosity in the fluid. Turbulent properties are compared

Table 1: Major characteristics of a turbulent tidal flow regime for different tidal stages identified in Fig. 4a.

	Vel. (m/s)		Turb. Str. (m/s)		Turb. int.	
Flow properties	<u>	<v>	σ_u	σ_v	I_u	I_v
I (flood flow)	0.9	0.1	0.04	0.04	0.05	0.35
II (flood flow)	1.25	0.15	0.07	0.06	0.06	0.37
III (ebb flow)	1.3	0.05	0.07	0.06	0.05	>1

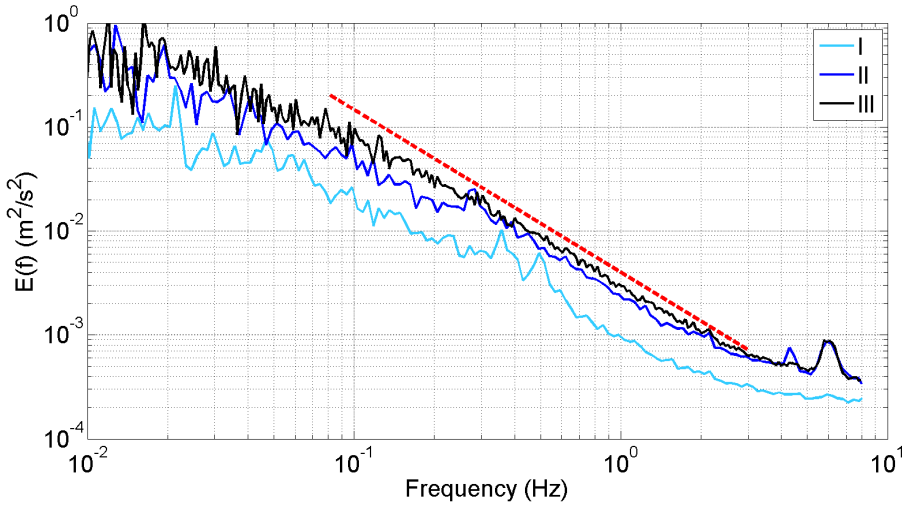

Figure 5: Power spectral density of the current velocity (streamwise component) during three specific periods of a tidal cycle identified in Fig. 4a and numbered I to III.

for different flow conditions: flooding tide with current velocity not exceeding 1 m/s, more energetic flood flow with velocity ranging from 1 to 1.5 m/s and also energetic ebbing tide with velocity close to 1.5 m/s (Fig. 4a). The major difference is found between two successive periods of flow evolution during the flood tide (periods I and II). The dissipation rate is found two times larger in the flow when the velocity exceeds 1 m/s. This velocity value represents a kind of threshold. Tidal stream with velocities higher than 1 m/s has much higher level of ambient turbulence and the change in turbulent regime is unexpectedly abrupt. The turbulent strength shown in Fig. 4a supports this assumption.

The second quantity evidencing a big change is the energy injection scale. It represents a typical size of turbulent eddies developed in the flow. The observations revealed that the size of such eddies increased by more than a factor of two, from 0.6 m to 1.6 m, between periods I and II (Tab. 2).

Finally, the estimates of Kolmogorov scale were found to be relatively stable, without a major change with respect to flow regimes. The smallest size of turbulent structures affected by viscous molecular diffusion of energy is estimated as $0.3 - 0.4$ mm which is a typical size for turbulent flow in rivers or in marine coastal environment.

3.3 Turbine performance

The bulk performance of the turbine is characterized by estimating the power coefficient, C_p, which is defined as a ratio of the output power generated by the turbine and the theoretical power, i.e. the

Table 2: Scaling properties of a turbulent flow for three characteristic periods of a tidal cycle in the Sea Scheldt, next to Antwerp (Belgium)

Scaling flow properties	$\epsilon(m^2s^{-3})$	$L(m)$	$\eta(m)$
I (flood flow)	1.2 10^{-4}	0.6	4.10^{-4}
II (flood flow)	2.3 10^{-4}	1.6	3.10^{-4}
III (ebb flow)	2.4 10^{-4}	1.5	3.10^{-4}

kinetic energy of the flow crossing the area swept by the blades:

$$C_p = \frac{P}{(1/2)\rho S u^3} \tag{6}$$

Here, ρ is the water density, S is the swept area, and u is the velocity in the approaching flow, assumed to be uniform over S. This assumption is valid, given the quasi-linear velocity profile in the uppermost surface layer (not shown).

The velocity values, derived from ADCP and 1-minute averaged, were used for assessing C_p. Space averaging of flow velocities was performed in the water layer $0.8 - 2$ m depth which is the layer occupied by the turbine ($0 - 2$ m). The output power, recorded at 100 Hz, was also 1-minute averaged and synchronized with the velocity measurements. Fig. 6a shows the distribution of the power coefficient (C_p) values, estimated within 1-minute intervals during successive turbine runs on flood flow, on November 7, 8, and 9 (Fig. 2b). The turbine rotation speed varied continuously with respect to the flow velocity and the pitch control enabled modulation of the rotation.

The optimum performance (max C_p) was reached for the flow velocity close to 1.2 m/s, yielding $C_{P_{\max}} \sim 0.42$ that is 71% of the highest theoretical performance. For lower current velocity values, $0.85 - 1$ m/s, the performance drops down to 0.30. Slightly higher C_p (0.33) is observed for even lower velocities ($0.6 - 0.85$ m/s), but the spreading of individual C_p estimates is also higher. The spreading in turbine performance estimates can result from variations of the torque exerted by the flow on the turbine, not steady pitch control of the blades, and presumably an electronic control of the load used in the experimental turbine runs.

The power curve (Fig. 6b) shows a gradual (linear) increase for velocity values ranging from 0.6 to 1.05 m/s. A considerable growth of power production is observed for higher velocities. The curve, obtained on the basis of 5-minute averaging, appears quite smooth and contains a very few outliers. It can be used for estimating the effective power production for different flow conditions at different sites.

3.4 Analysis of power production and a relationship with turbulence in the tidal flow

While the turbine performance reaches its optimal value for current velocities higher than 1.1 m/s, the power production suffers from the lack of stability and becomes strongly intermittent. Fig. 7a gives an example of such intermittency and reveals a larger level of fluctuations of power for this velocity

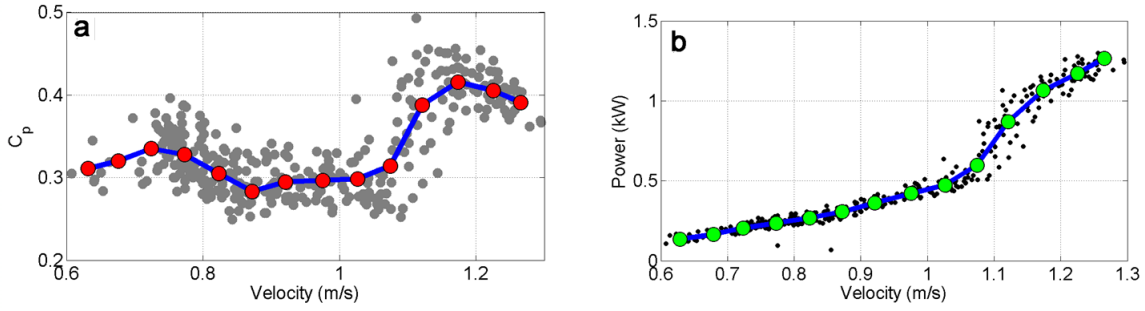

Figure 6: (a) Performance coefficient C_p values estimated on a basis of 1-minute averarging (grey dots) of the output power and the theoretical power. Red dots represent C_p values averaged within 0.05 m/s velocity intervals. (b) Power curve of the vertical axis tidal turbine "W2E". Black dots show 1-minute averaged power and green dots represent mean power values for 0.05 m/s velocity intervals.

range. The output power variability results from variations of torque due to turbulent character of the flow which exerts highly irregular load on the blades.

To investigate the coupling between the instantaneous turbine response and turbulence in the approach flow, a joint analysis of the scaling properties of the tidal flow and the output power is performed. Fig. 8 shows the PSD of the power time series recorded at 100 Hz on November 7 during a 3-hour test run of the W2E turbine. Three characteristic regions are identified in the spectrum of the output power P. In low-frequency band ($f_b < 4.10^{-2}$ Hz), power fluctuations seem to be decoupled from velocity fluctuations (Fig. 5). The spectral slope for power is different, the spectral curve tends to flatten and shows strong variations of PSD.

In the inertial sub-range (4.10^{-2} Hz $< f <$ 2 Hz) the turbine output power appears to be conditioned by the turbulent energy cascade in the tidal flow. The PSD of the output power shows scaling similar to that obtained for velocities in the approaching flow (Fig. 8 and Fig. 5). Spectral slope is very close -5/3 for both quantities.

In the sub-range $f > 4.10^{-1}$ Hz (max f), the shape of the spectrum for power is largely distorted and reveals that power fluctuations are globally concentrated in two frequencies f_0 and $4f_0$, where f_0 denotes the turbine frequency. The higher harmonic, $4f_0$, evidences a strong interaction of each of four turbine blades with the incident flow. Both frequencies lie within the inertial sub-range where the turbine is assumed to "actively" interact with the turbulent flow.

In the high frequency region ($f >$ 5 Hz), the turbine power fluctuations appear to be non-responsive to turbulent motions. Above the critical frequency f_c = 4 Hz, both the output power and velocity fluctuations loose nice scaling. Velocity fluctuations are affected by noise and interpretation of flow variability is difficult in this frequency band (Fig. 5). The spectral slope of the output power also flattens, more clearly for power generated during the period I (lower power) than during the period II (higher power). For both periods, the power records seem to be affected by noise in this spectral band.

Comparison of the output power spectra for period I and II, corresponding to periods of lower and higher mean flow velocity, reveals a large difference in the magnitude of power fluctuations. Fig. 8 shows the difference of more than one decade between two PSD curves. The magnitude of power vari-

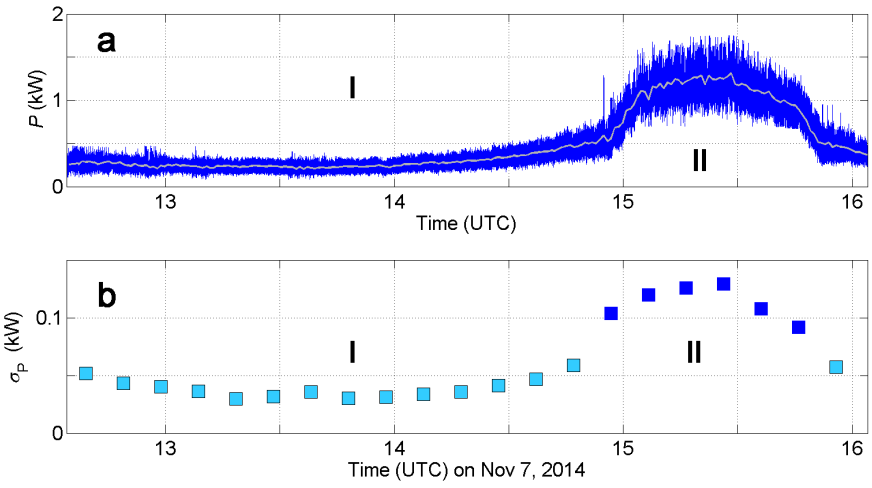

Figure 7: (a) Power generated by the VATT - W2E - during the test run on November 7, 2014. One second averaged time series of the power recorded at 100 Hz is given in blue. One minute averaged power is given in grey. (b) Standard deviation of power fluctuations within 10-min intervals. Periods of moderate and high current velocity are denoted by I and II, and also by light and dark blue.

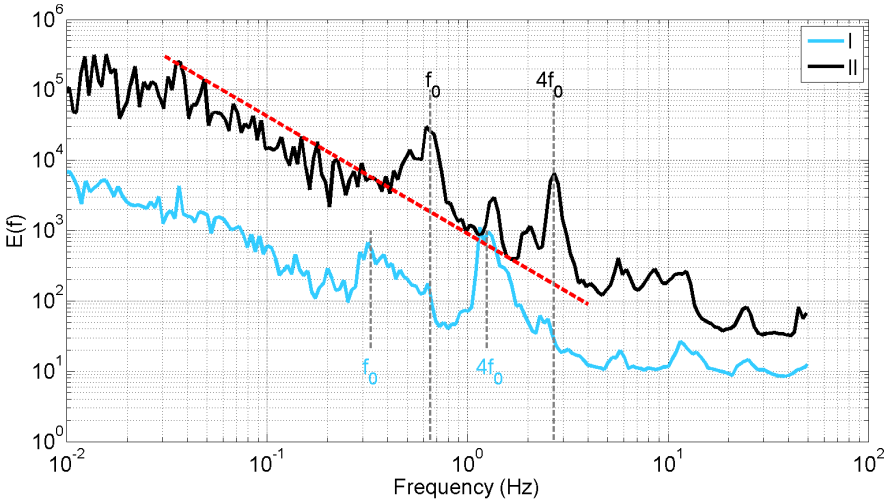

Figure 8: Power spectral density of the output power generated by the turbine on November 7, 2014, during two periods of the flood tide identified in Fig. 7 and numbered I and II. Red line shows the spectral slope $f^{-5/3}$. The mean frequency of turbine rotation is given by f_0 for each period.

ability can also be quantified by estimating the standard deviation (std) of power fluctuations for specific periods. Fig. 7b shows that the standard deviation of the output power increased more than two times (from 0.05 to 0.12 kW) during the period II. Both representations (spectral and statistic) revealed a tight relationship between the variability of the output power and the turbulence in the tidal stream in the inertial sub-range (Fig. 4, 5 and Fig. 7, 8). The spectral representation of the power and flow velocity variability shows similar scaling in this sub-range.

Estimation of the fundamental turbulent properties of the flow (Tab. 2) shows that the dissipation rate is two times higher during the period II. Moreover, the size of turbulent eddies in the tidal stream considerably increased between two periods (up to 1.6 m) and became comparable with the turbine size (2 x 1.5 m).

This result provides important insights into the dynamics of the turbine response to variable flow regimes and particularly to the level of ambient turbulence in the flow. In an energetic tidal flow with velocities higher than 1 m/s, the turbulent kinetic energy is cascading from larger eddies of size L = 1.6 m to smaller eddies of size less than one mm (η) and then dissipates as a heat. Turbulent eddies of large size exert periodic loads on the blades, strongly affect torque and cause power pulsations. The magnitude of such pulsations is very high. PSD distribution shows a considerable increase of the magnitude by more than one decade, corresponding to two frequencies f_0 and $4f_0$ (Fig. 8).

In the real tidal flow conditions, turbulence is the major factor responsible for the intermittency of power production by a free-stream tidal turbine. Turbulence intensity I_u, used by engineers to quantify the level of ambient turbulence, does not appear to be appropriate metric as it can not capture a quantitative change of the turbulent flow regime during the tidal flow transition from lower to higher velocities. Other metrics, such as dissipation rate, ϵ, and energy injection scale, L, appears more appropriate for turbulence characterization.

During the period II, higher level of ambient turbulence causes stronger variability of power production by exerting loads on the blades which in turn produces strong variations of torque. The spectral representation of the power and flow velocity variability shows similar scaling in the inertial sub-range. Variations of the output power show similar evolution and are assumed to be caused by turbulent eddies of size comparable with the turbine size.

4 Concluding remarks

In summary, our results highlight the advantage of using multiple instrument techniques to assess the turbulence properties at tidal energy sites and the impact of turbulence on the output power. Continuous ADCP measurements of flow velocity provide the good quality data and allow evaluating the turbine performance. For the tested VATT, the optimal performance (C_p) attained 0.42 in the velocity range $1.1-1.2$ m/s.

However ADCP does not allow an accurate assessment of the current intermittency which is crucial for understanding the output power variability. ADV measurements, performed at test site, demonstrated that the dissipation rate, ϵ, and turbulent strength, σ_u, are the preferred metrics for characterizing the turbulence. They are tightly related with the magnitude of the output power variability and provide an insight on very probable interaction between the turbulence in the flow and the VATT. Specifically, it was demonstrated that tidal turbine responds more actively to turbulence on scales similar to the rotor diameter.

In real tidal stream, characterized by a limited range and continuously varying flow speed, turbulent intensity does not change much with increasing mean speed and therefore does not seem to be an adapted metric for understanding the interaction between the tidal turbine and the turbulence.

ADV survey should be performed at tidal energy site prior to turbine testing. High frequency and high quality data provided by ADV can help to find an optimal design and size of turbines in order to minimise an extra load on the blades considered as the major source of fatigue. This is our recommendation to community of engineers involved in tidal energy conversion projects. Given the complexity of the problem, more experiments in real sea conditions are required for better understanding of the reach interaction between an intermittent flow and the power production by tidal turbines.

Acknowledgment

The authors would like to acknowledge the support of the Interreg IVB (NW Europe) "Pro-Tide" Project. The authors also ackowledge Reiner Rijke (Water2Energy) for supplying the output power data recorded during tidal turbines testing and Roeland Notele (SeaKanal) for offering technical support during the fieldwork. The experience of Eric Lecuyer (technician in LOG) and his help during the fieldwork are appreciated and acknowledged.

References

[1] L. S. Blunden and A. S. Bahaj, "Tidal energy resource assessment for tidal stream generators," *Proceedings of the Institution of Mechanical Engineers, Part A: Journal of Power and Energy*, vol. 221, no. 2, pp. 137–146, 2007.

[2] U. Frish, *The legacy of A.N. Kolmogorov*. Cambridge University Press, 1995.

[3] P. Mycek, B. Gaurier, G. Germain, G. Pinon, and E. Rivoalen, "Experimental study of the turbulence intensity effects on marine current turbines behaviour. Part II: Two interacting turbines," *Renewable Energy*, vol. 68, pp. 876–892, 2014.

[4] L. P. Chamorro, C. Hill, S. Morton, C. Ellis, R. E. A. Arndt, and F. Sotiropoulos, "On the interaction between a turbulent open channel flow and an axial-flow turbine," *Journal of Fluid Mechanics*, vol. 716, pp. 658–670, 2013.

[5] W. M. J. Batten, A. S. Bahaj, A. F. Molland, and J. R. Chaplin, "The prediction of the hydrodynamic performance of marine current turbines," *Renewable Energy*, vol. 33, no. 5, pp. 1085–1096, 2008.

[6] G. Pinon, P. Mycek, G. Germain, and E. Rivoalen, "Numerical simulation of the wake of marine current turbines with a particle method," *Renewable Energy*, vol. 46, pp. 111–126, 2012.

[7] A. S. Bahaj, A. F. Molland, J. R. Chaplin, and W. M. J. Batten, "Power and thrust measurements of marine current turbines under various hydrodynamic flow conditions in a cavitation tunnel and a towing tank," *Renewable energy*, vol. 32, no. 3, pp. 407–426, 2007.

[8] F. Maganga, G. Germain, J. King, G. Pinon, and E. Rivoalen, "Experimental characterisation of flow effects on marine current turbine behaviour and on its wake properties," *IET Renewable Power Generation*, vol. 4, no. 6, p. 498, 2010.

[9] J. MacEnri, M. Reed, and T. Thiringer, "Influence of tidal parameters on SeaGen flicker performance," *Philosophical Transactions of the Royal Society of London A: Mathematical, Physical and Engineering Sciences*, vol. 371, no. 1985, p. 20120247, 2013.

[10] P. Jeffcoate, R. Starzmann, B. Elsaesser, S. Scholl, and S. Bischoff, "Field measurements of a full scale tidal turbine," *International Journal of Marine Energy*, vol. 12, pp. 3–20, 2015.

[11] J. Thomson, B. Polagye, V. Durgesh, and M. C. Richmond, "Measurements of turbulence at two tidal energy sites in Puget Sound, WA," *Oceanic Engineering, IEEE Journal of Oceanic Enginnering*, vol. 37, no. 3, pp. 363–374, 2012.

[12] K. Korotenko, A. Sentchev, F. G. Schmitt, and N. Jouanneau, "Variability of turbulent quantities in the tidal bottom boundary layer: Case study in the eastern English Channel," *Continental Shelf Research*, vol. 58, pp. 21–31, 2013.

[13] K. McCaffrey, B. Fox-Kemper, P. E. Hamlington, and J. Thomson, "Characterization of turbulence anisotropy, coherence, and intermittency at a prospective tidal energy site: Observational data analysis," *Renewable Energy*, vol. 76, pp. 441–453, 2015.

[14] P. J. Wiles, T. P. Rippeth, J. H. Simpson, and P. J. Hendricks, "A novel technique for measuring the rate of turbulent dissipation in the marine environment," *Geophysical Research Letters*, vol. 33, no. 21, 2006.

[15] J. Thomson, B. Polagye, M. Richmond, and V. Durgesh, "Quantifying turbulence for tidal power applications," in *OCEANS 2010*. IEEE, 2010, pp. 1–8.

[16] I. A. Milne, R. N. Sharma, R. G. J. Flay, and S. Bickerton, "Characteristics of the turbulence in the flow at a tidal stream power site," *Philosophical Transactions of the Royal Society of London A: Mathematical, Physical and Engineering Sciences*, vol. 371, no. 1985, p. 20120196, Feb. 2013.

[17] S. B. Pope, *Turbulent flows*. Cambridge University Press, 2000.